

# Supramolecular structure of highly oriented wet-spun polyacrylonitrile fibers used in the preparation of high-performance carbon fibers

Qin Ouyang<sup>1</sup> · Yousi Chen<sup>1</sup> · Xuefei Wang<sup>1</sup> · Hongbo Ma<sup>1</sup> · Dehong Li<sup>1</sup> · Jianxing Yang<sup>1</sup>

Received: 7 July 2015 / Accepted: 19 October 2015 / Published online: 4 November 2015  
© Springer Science+Business Media Dordrecht 2015

**Abstract** Highly oriented polyacrylonitrile (PAN) fibers, which are used in the preparation of high-performance carbon fibers, were prepared via a wet spinning process. The supramolecular structure—i.e., the degree of crystallinity, crystal size, and crystallite orientation—of the PAN fibers was characterized by X-ray diffraction (XRD) using fiber and powder techniques. Two equatorial diffraction peaks with  $2\theta \sim 17^\circ$  and  $29.5^\circ$  were observed in the fiber XRD patterns, which confirmed that the crystalline structure of the PAN fibers was pseudo-hexagonal with only two-dimensional order in the transverse direction. The powder XRD patterns were resolved into three constituent Lorentz peaks to determine the relative degree of crystallinity. In order to increase the reproducibility of the value for the crystallinity of the fibers, the Gupta–Singhal method was modified by assuming that the degree of crystallinity could be determined from the area under peak 1 (with  $2\theta \sim 17^\circ$ ), rather than the combined area of peaks 1 and 3. The evolution of the supramolecular structure of the PAN fibers during the spinning process was also investigated. Results indicated that drying and steam stretching play important roles in the formation and growth of the crystalline structure of the PAN fibers, while the orientation of the structure was only strongly related to the degree of stretching. The effects of the supramolecular structure on the thermal properties and mechanical properties of the PAN fibers were also studied. The perfection of the supramolecular structure influenced the feasibility of cyclization reactions within the

PAN fibers and the thermal decomposition of those fibers. The mechanical properties of the PAN fibers were significantly enhanced by increasing the perfection of the supramolecular structure.

**Keywords** Polyacrylonitrile fiber · Supramolecular structure · Crystallinity · Orientation · Carbon fiber

## Introduction

Polyacrylonitrile (PAN) is currently the most important precursor for carbon fibers [1]. Due to their excellent and balanced mechanical properties, PAN-based carbon fibers have been widely applied in various fields, such as in sporting goods, aircraft, the aerospace industry, automobiles, pressure containers, and windmill blades [1–3]. Producing PAN-based carbon fibers involves the following steps: polymerization, spinning, thermal stabilization, and carbonization. The supramolecular structure—i.e., the degree of crystallinity, crystal size, and crystallite orientation—of the PAN fibers formed during the spinning process is directly related to the mechanical properties of the PAN fibers, and plays an important role in their subsequent structural transformation into carbon fibers [3, 4]. The supramolecular structure of the PAN fibers dramatically influences the cyclization reactions and shrinkage that occur during thermal stabilization due to its effect on the thermal mobility of the PAN chains [5].

Many investigations have been performed to improve our understanding of the nature of the supramolecular structure of PAN [6–15]. However, there is still a lack of clarity, especially about the crystalline structure of PAN. Some authors have even questioned whether the order observed in the structure of PAN should be termed “crystalline” [6, 7]. The central issue of this argument is the phase morphology of PAN. In

✉ Qin Ouyang  
o\_yang@126.com; ouyangqin@nimte.ac.cn

<sup>1</sup> National Engineering Laboratory for Carbon Fiber Preparation Technology, Ningbo Institute of Material Technology & Engineering, Chinese Academy of Sciences, Ningbo 315201, China

1961, Bohn et al. proposed that PAN was a single-phase, laterally ordered polymer with a planar unit cell, and that it formed a two-dimensional crystal or a paracrystal [6]. Subsequently, Holland et al. [8] and Klement and Geil [9] reported that single crystals of PAN could be grown from dilute propylene carbonate solution at 90–100 °C over the course of several days, and that electron and X-ray diffraction results indicated that these crystals possess lateral order. Henrici-Olivé and Olivé further assumed that PAN chains have a rigid and irregular helical conformation due to the intramolecular repulsion of adjacent nitrile groups [10]; the rod-like PAN chains are packed together hexagonally and display lateral order but disorder along the *c*-axis. However, it is still unclear whether the packing of PAN chains is hexagonal or orthorhombic, whether PAN has two-dimensional or three-dimensional order, and whether the morphology of PAN is two-phase or single-phase [6–15].

In 1979, Warner and Uhlmann [11] presented a two-phase model for the structure of oriented PAN fibers. It was suggested that the PAN chains form fibrils with two distinct regions: an amorphous (disordered) region and a partially ordered region. The partially ordered region was similar to Bohn's model in that the rods of contorted helical PAN chains were parallel to the fiber axis. The disordered region consisted of loops, folds, entanglements, chain ends, defects, etc. [11]. In 2005, Bashir and Rastogi reported that the unoriented PAN had a two-phase morphology (ordered plus amorphous), but that oriented PAN had only a single-phase morphology (i.e., it is only ordered) [12, 13]. In addition, based on X-ray diffraction (XRD) results, they proposed that the ordered phase in PAN was not crystalline but a mesophase glass [12]. In 2006, Bai et al. examined the microstructure of PAN fibers by high-resolution transmission electron microscopy (HRTEM) and observed an unusual phenomenon: the coexistence of ordered and amorphous phases [14]. They claimed that crystallite structures (onion-like spheres) predominated in the transverse section, whereas highly oriented structures (ribbons) were dominant in the longitudinal sections. In another of their studies, they even observed nanocrystallites and two types of amorphous microstructures (onion-like spheres and maze-like matrices) in the PAN fibers [15].

As can be seen from the above review, although various characteristics and models have been proposed for the supramolecular structure of PAN, they do not appear to agree with each other. This can be attributed to the use of PAN samples in different states (such as dry or wet and powder, membrane, or fiber) in the various studies and the application of different investigative tools by the researchers [such as wide-angle X-ray diffraction (WAXD), small-angle X-ray scattering (SAXS), differential scanning calorimetry (DSC), dynamic mechanical analysis (DMA), and high-resolution transmission electron microscopy (HRTEM)]. The supramolecular structure of PAN is strongly dependent on the processing

conditions. Preparing PAN fibers for use in the preparation of high-performance carbon fibers requires several steps, including coagulation, washing, and stretching in water baths, finishing with oil agents, drying and densification, and then stretching and relaxing in water steam to decrease the diameter and increase the orientation of the PAN fibers. Each step in the spinning process plays an important role in developing the supramolecular structure of the PAN fibers.

In the study reported in the present paper, highly oriented PAN fibers (as used in the preparation of high-performance carbon fibers) were prepared via a wet spinning technique. The supramolecular structure of the PAN fibers was characterized by XRD using fiber and powder techniques. The evolution of the supramolecular structure of the PAN fibers during the spinning process was investigated to ascertain the factors that influence this structure. The effect of the supramolecular structure on the thermal properties of the PAN fibers was also studied by DSC and TG analysis.

## Experimental

### Materials

Acrylonitrile (AN), purchased from Zhejiang Taizhou Zhonghai Pharmaceutical & Chemical Co., Ltd. (Taizhou City, China), was purified before use by vacuum distillation to remove the inhibitor. Itaconic acid (IA) with a concentration of 99 %, which was purchased from Aldrich Chemical Co., Inc. (St. Louis, MO, USA), was used without further purification. Dimethylsulfoxide (DMSO) and  $\alpha,\alpha'$ -azobisisobutyronitrile (AIBN) were both commercial products and used as received.

### Sample preparation

The PAN fibers were prepared via a wet spinning process. A spinning solution of PAN was prepared via homogeneous free-radical copolymerization of AN and about 2 wt% IA (used as the comonomer) in DMSO, followed by the removal of the unreacted AN and deaeration. The PAN spinning solution was extruded into a DMSO/H<sub>2</sub>O mixture used as a coagulation bath. The coagulated PAN fibers were washed and stretched successively in water baths at different temperatures (ranging from 50 to 90 °C) and then finished by immersion in an oil agent (an oil-in-water emulsion) for isolation and protection. Subsequently, the wet PAN fibers were dried at elevated temperatures of 100–150 °C. During this process, water was removed and the voids in the fibers collapsed, resulting in a dense structure. Finally, the PAN fibers were treated in two high-temperature water steam machines by stretching and relaxing them successively to greatly increase the level of orientation and eliminate the internal stress. To investigate the evolution of the supramolecular structure of the PAN

fibers during the spinning process, four PAN fiber samples (nos. 1–4) were collected at successive stages during the spinning process (shown in Fig. 1) and analyzed.

In order to permit a comparison with the supramolecular structure of the highly oriented PAN fibers, an unoriented PAN polymer was prepared by heterogeneous free-radical copolymerization of AN with about 2 wt% IA (used as a comonomer) in a DMSO/H<sub>2</sub>O mixture (w/w 50:50) using AIBN as initiator at 60 °C. The unoriented PAN polymer sample was obtained by washing, drying, and grinding after the polymerization reaction.

**Characterization**

A Quanta FEG 250 (FEI, Hillsboro, OR, USA) scanning electron microscope (SEM) was used to characterize the surface and cross-sectional morphology of the PAN fibers, which were coated with Pt before observation.

The powder XRD patterns of the finely powdered PAN fiber and polymer samples were recorded on a D8 Advance X-ray diffractometer (Bruker, Karlsruhe, Germany) operated at a voltage of 40 kV and a current of 40 mA using nickel-filtered Cu K-α radiation (wavelength: 0.154 nm). The continuous scan method used had a scanning range of 10–35° (2θ) with a scanning speed of 1° per minute. The XRD patterns were resolved into constituent Lorentz peaks of crystalline

(peak area: *A<sub>c</sub>*) and amorphous (peak area: *A<sub>a</sub>*) phases using the peak fitting module (PFM) of Origin Pro 7.5 (OriginLab Co., Northampton, MA, USA). A linear line was drawn between 2θ=10 and 35° for baseline subtraction. The crystallinity *C* was determined using the areas of the deconvoluted peaks:

$$C = \frac{A_c}{A_c + A_a} \times 100\% \tag{1}$$

The intense peak at 2θ ~ 17° was used to calculate the crystalline parameters, plane spacing (*d*), and lateral crystal size (*L*) using Bragg’s formula and the Scherrer equation, respectively. In the Scherrer equation, *K*=0.9 and β is the full width at half maximum intensity (FWHM).

$$d = \frac{\lambda}{2 \sin \vartheta} \tag{2}$$

$$L = \frac{K\lambda}{\beta \cos \vartheta} \tag{3}$$

The fiber XRD patterns of the PAN fiber samples were obtained on an X’Pert PRO X-ray diffractometer

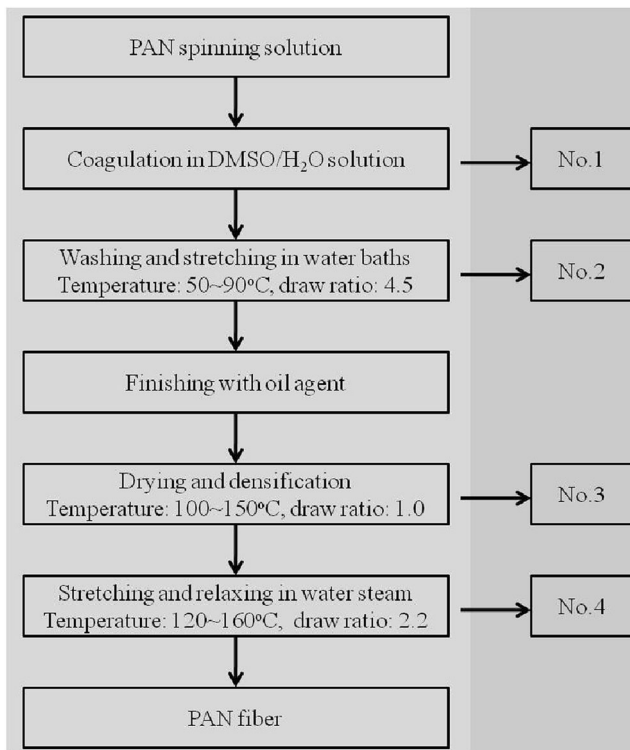


**Fig. 1** Schematic showing the successive stages of the fiber spinning process during which PAN fiber samples were taken

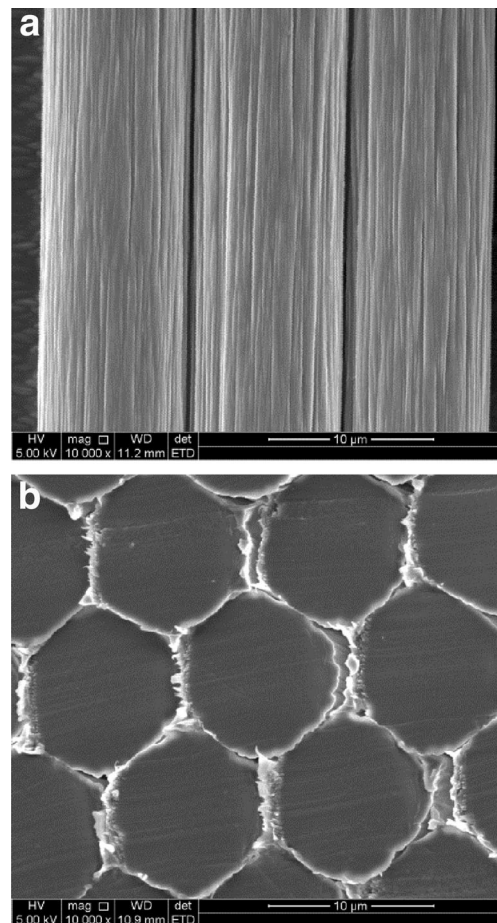


**Fig. 2a–b** SEM images of PAN fiber sample no. 4: **a** surface; **b** cross-section

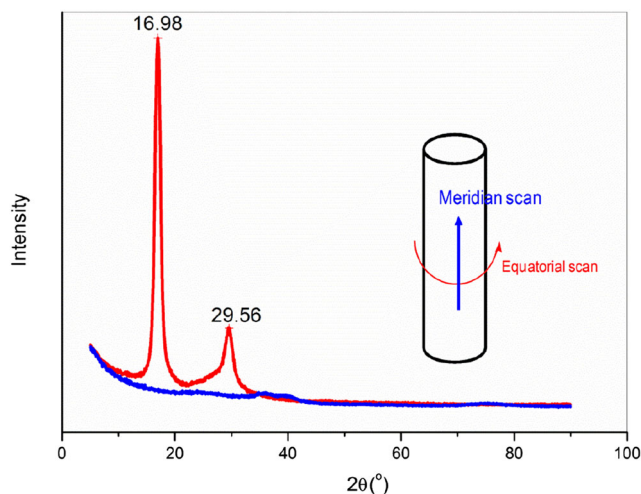


**Fig. 3** XRD patterns for PAN fiber sample no. 4, as obtained by scanning in different directions

(PANalytical, Almelo, Netherlands) with nickel-filtered Cu K- $\alpha$  radiation ( $\lambda=0.154$  nm, 40 kV, 40 mA). The PAN fiber samples were arranged parallel to each other on a fiber specimen attachment. Measurements were made by performing equatorial scans (perpendicular to the fiber axis) and meridian scans (parallel to the fiber axis), as well as azimuthal scans (rotating the fibers in the attachment). The orientation measurements were carried out using azimuthal scans at  $2\theta \sim 17^\circ$ , corresponding to (100) reflection. The dependence of the diffraction intensity on the azimuthal angle was well fitted by a Gaussian function using the peak fitting module (PFM) of OriginPro 7.5. The FWHM,  $H$ , of the azimuthal scan curve was used to calculate the degree of orientation  $\pi$  [16]:

$$\pi = \frac{180 - H}{180} \times 100\% \quad (4)$$

DSC/TG analysis of the PAN fiber samples was carried out using a Netzsch (Selb, Germany) STA 449 thermal analyzer under a nitrogen atmosphere at a heating rate of  $10^\circ\text{C min}^{-1}$  from room temperature to  $500^\circ\text{C}$ .

Stress-strain curves of the PAN fibers were obtained by a monofilament method with a Donghua University (Shanghai,

China) XQ-1/XD-1 single-fiber tester. Each mechanical property was reported as the average value of multiple test results, and the relative standard deviation (namely the coefficient of variation, CV) was also calculated.

## Results and discussion

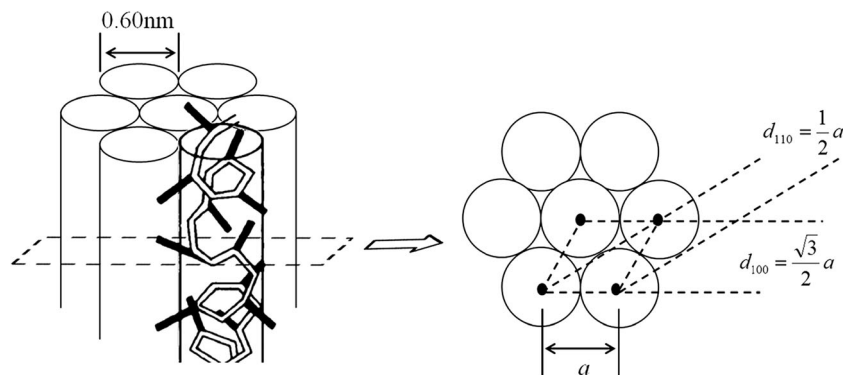
### Characterization of the surface and cross-sectional morphology of the PAN fibers by SEM

Figure 2 shows SEM images of PAN fiber sample no. 4. It is clear that there are a lot of grooves in the surfaces of the PAN fibers. These characteristic grooves are associated with the wet spinning process employed. They are generated when the fibrillar network structure that is formed by phase separation during coagulation collapses [16]. As can be seen from Fig. 2a, the grooves are strongly oriented along the fiber axis. This indicates that the PAN fibers have a high degree of orientation. As shown in Fig. 2b, the PAN fibers have circular cross-sections and dense internal structure. There are no voids or other defects in the surfaces and cross-sections of the PAN fibers. This PAN fiber morphology is necessary if they are to be used in the preparation of high-performance carbon fibers.

### Characterization of the crystalline structure of the PAN fibers by XRD

Figure 3 shows XRD patterns of PAN fiber sample no. 4 obtained by performing equatorial and meridian scans. In the equatorial pattern, a sharp diffraction peak at  $2\theta=16.98^\circ$  and a small diffraction peak at  $2\theta=29.56^\circ$  are observed. However, no distinct diffraction peak is apparent in the meridian pattern. This indicates that the PAN fibers only possess two-dimensional order in the transverse direction, with no order present in the longitudinal direction. Previous reports of the diffraction pattern of PAN also generally found only two equatorial peaks [12, 17]. The  $d$  spacings corresponding to the two equatorial peaks, as calculated using the Bragg equation, are 0.52 nm and 0.30 nm, respectively. The ratio of these two  $d$

**Fig. 4** Schematic of the pseudo-hexagonal crystalline structure of PAN



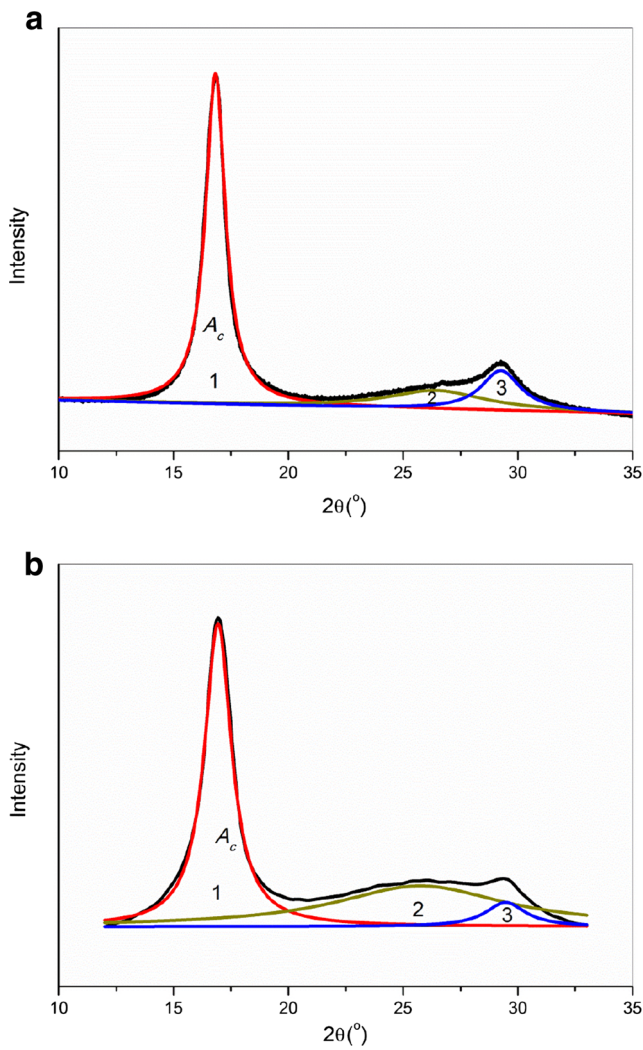


**Fig. 5a–b** Powder XRD patterns of PAN samples resolved using PFM: **a** PAN fiber sample no. 4; **b** PAN polymer

spacings is 1.733. The  $d$  spacing for hexagonal packing ( $d_{hkl}$ ) can be calculated as follows:

$$\frac{1}{d_{hkl}^2} = \frac{4}{3} \left( \frac{h^2 + hk + k^2}{a^2} \right) + \frac{l^2}{c^2} \tag{5}$$

Therefore,  $d_{100} = a\sqrt{3}/2$ ,  $d_{110} = a/2$ , and the ratio  $d_{100}/d_{110}$  is  $\sqrt{3}$ . Since  $\sqrt{3} \approx 1.732$ , which is very close to the ratio of the

two equatorial  $d$  spacings for the PAN fiber, we can confirm that the crystalline structure of the PAN is hexagonal, or—more exactly—it is pseudohexagonal with two-dimensional order.

As shown in Fig. 4, the rod-like PAN chains are packed together hexagonally, and the diameter of each rod is  $2d_{110}$ , i.e., 0.60 nm. According to Henrici-Olivé and Olivé, each PAN chain has a rigid and irregular helical conformation due to the intramolecular repulsion of adjacent nitrile groups [10]. Although this irregular helical conformation of PAN chains is widely accepted by most people, some other researchers believe that each PAN chain has a planar zigzag conformation [17]. Actually, these two types of conformation probably co-exist in PAN fibers. As assumed by Chae et al., the proportion of planar zigzag chains would increase with increasing draw ratio [18]. Theoretically, the planar zigzag conformation is more conducive to intramolecular cyclization reactions of adjacent nitrile groups during thermal stabilization, leading to the formation of a more heat-stable ladder structure.

**Determination of the relative degree of crystallinity of the PAN fibers by powder XRD**

Figure 5a and b show powder XRD patterns of PAN fiber sample no. 4 and the polymer, respectively. Both the PAN fibers and the polymer exhibit a rather strong and relatively sharp peak at about  $2\theta = 16.9^\circ$ , a broad diffuse scattering maximum situated around  $2\theta = 20\text{--}30^\circ$ , and a weak peak at about  $2\theta = 29.5^\circ$ . These peaks are labeled peak 1, peak 2, and peak 3, respectively, in Fig. 5. Peaks 1 and 3 are attributed to the two reflections of the crystalline phase, whereas peak 2 is attributed to a reflection from the amorphous phase [19]. The relative degree of crystallinity of PAN is generally evaluated by separating the total area of the XRD pattern into crystalline and amorphous components. Three methods have been devised to calculate the relative degree of crystallinity of PAN from an XRD pattern: the Hinrichsen method [20], the Bell–Dumbleton method [21], and the Gupta–Singhal method [19]. All of these methods require the separation of the XRD pattern into contributions from the crystalline and amorphous phases, as discussed in detail in the literature [19]. Among these methods, the Gupta–Singhal method, involving

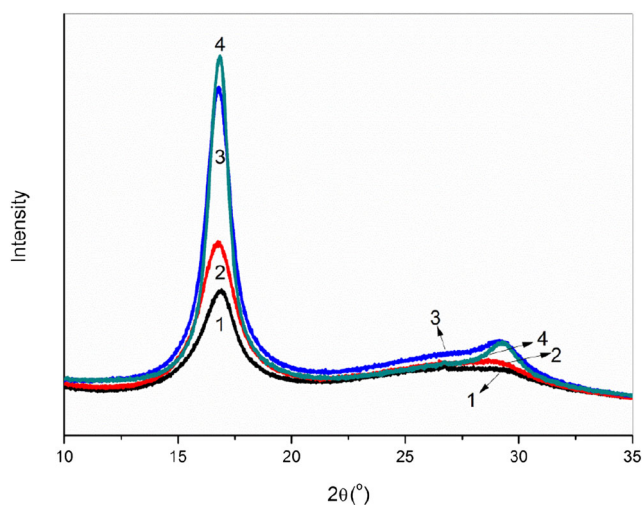
**Table 1** Characteristics of the peaks resolved from the powder XRD patterns of PAN samples

Sample	Peak	Center	FWHM	Area percentage	Crystal size	Degree of crystallinity
PAN fiber sample no.4	1	16.83°	1.05°	67.64 %	7.7 nm	67.64 %
	2	26.44°	5.23°	16.83 %		
	3	29.26°	2.09°	15.53 %		
PAN polymer	1	16.94°	1.44°	56.77 %	5.6 nm	56.77 %
	2	25.74°	9.10°	36.94 %		
	3	29.46°	2.10°	6.29 %		

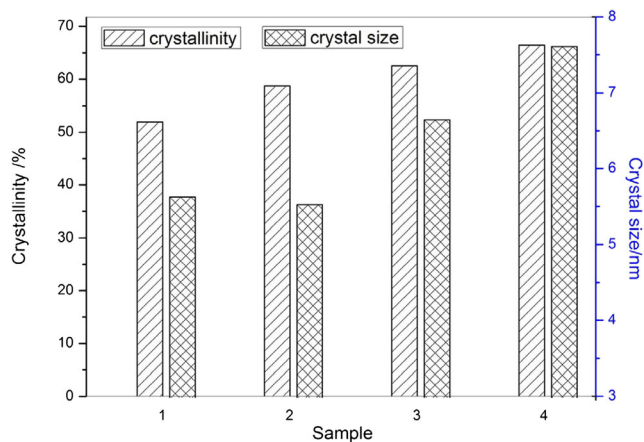
resolution of the symmetrical individual maxima in the XRD pattern, seems to be more reasonable than the other two methods.

In order to divide the total area of the XRD pattern into crystalline and amorphous components, a computer-aided curve-resolution technique was used to separate the crystalline and amorphous phases [22, 23]. In this work, the XRD patterns were resolved using the peak fitting module (PFM) in the Origin Pro 7.5 software. First, a baseline was defined and the area under the baseline was subtracted from the diffraction pattern. Then the residual pattern was resolved into the three constituent Lorentz peaks using PFM by keeping the peak positions largely constant and requiring that the total area of the resolved peaks best approximates the area of the experimental diffraction pattern.

Gupta and Singhal [19] considered the total area under resolved peaks 1 and 3 to be  $A_c$  and the area under peak 2 to be  $A_a$ . However, although peak 1 was easy to resolve from the diffraction pattern with reasonable precision, we found the repeatability of the resolution of peaks 2 and 3 to be very poor because they overlap and were often inseparable. Since the area of peak 3 was small, in order to obtain a more reproducible value for the degree of crystallinity, we modified the Gupta–Singhal method by considering only the area under resolved peak 1 to be  $A_c$  and the remaining area to be  $A_a$ . Based on the Bell–Dumbleton method, the area of peak 3 was also excluded from  $A_c$  for the sake of convenience and to improve repeatability [21]. As long as peak 1 was resolved from the diffraction pattern, the relative degree of crystallinity  $C$  could be obtained and the crystal size  $L$  could be calculated using the Scherrer equation. The results for the PAN fiber and polymer are listed in Table 1. The highly oriented PAN fibers have higher  $C$  and  $L$  values than the unoriented PAN polymer, which can be attributed to the increased degree of orientation of the PAN chains [24].



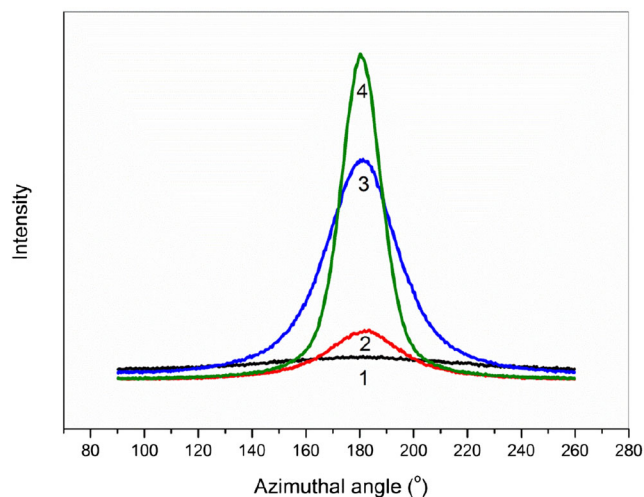
**Fig. 6** Powder XRD patterns of the PAN fiber samples



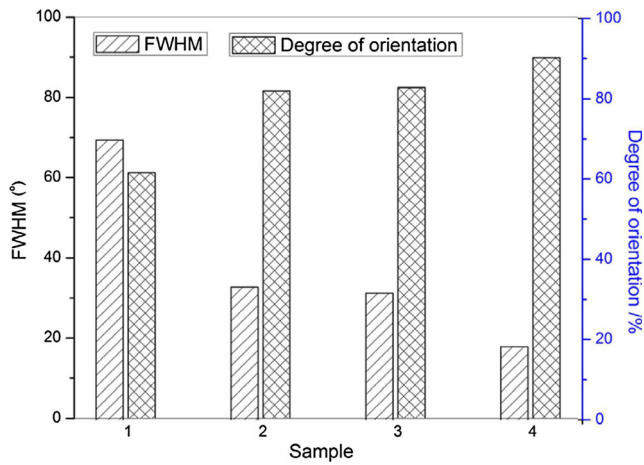
**Fig. 7** Crystallinities and lateral crystal sizes of the PAN fiber samples

### Evolution of the crystalline structure of the PAN fibers during the spinning process

Figure 6 shows the powder XRD patterns of PAN fiber samples obtained at different stages during the spinning process. As shown in Fig. 6, all of the XRD patterns exhibit a rather strong peak at about  $2\theta=17^\circ$  and a broad diffuse scattering maximum situated around  $2\theta=20\text{--}30^\circ$ . In sample nos. 1 and 2, the diffraction peak at about  $2\theta=17^\circ$  is very broad, and the diffraction peak at about  $2\theta=29.5^\circ$  disappears into the broad diffuse scattering peak. It has been suggested that, at these two stages, the crystalline structure of PAN fibers is still imperfect, which is probably due to the hindrance exerted by voids and small molecules such as water and solvent among the PAN chains [16]. After drying and collapsing, the diffraction peak at about  $2\theta=17^\circ$  becomes very sharp and strong. It becomes even stronger after stretching and relaxing the fibers in steam, and the diffraction peak at about  $2\theta=29.5^\circ$  also becomes apparent. This means that the perfection of the crystalline structure of the PAN fibers increases.



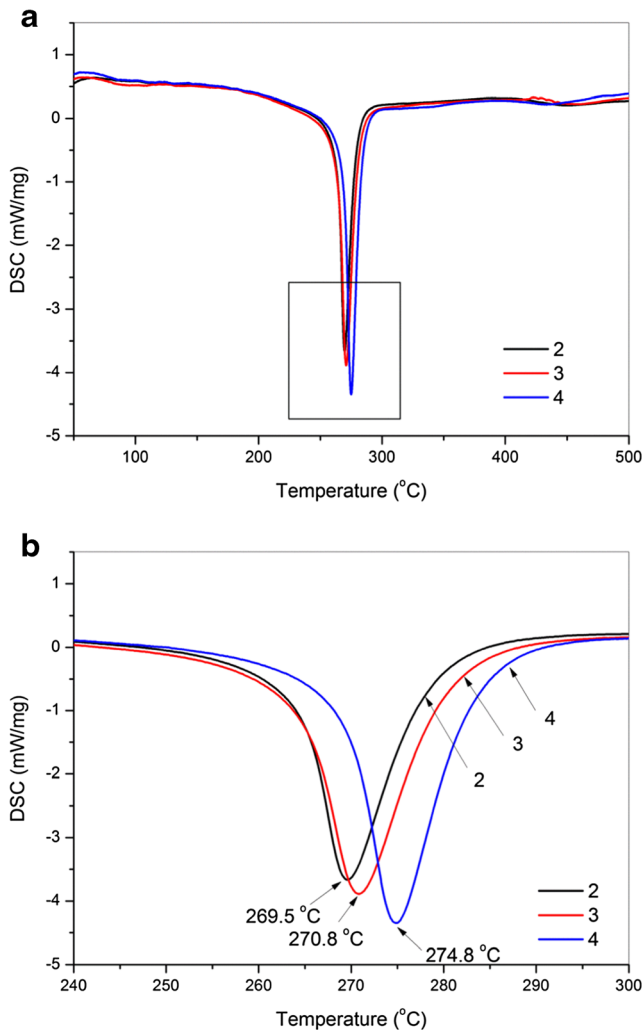
**Fig. 8** Fiber XRD patterns of the PAN fiber samples, as obtained by azimuthal scans at  $2\theta = 17^\circ$



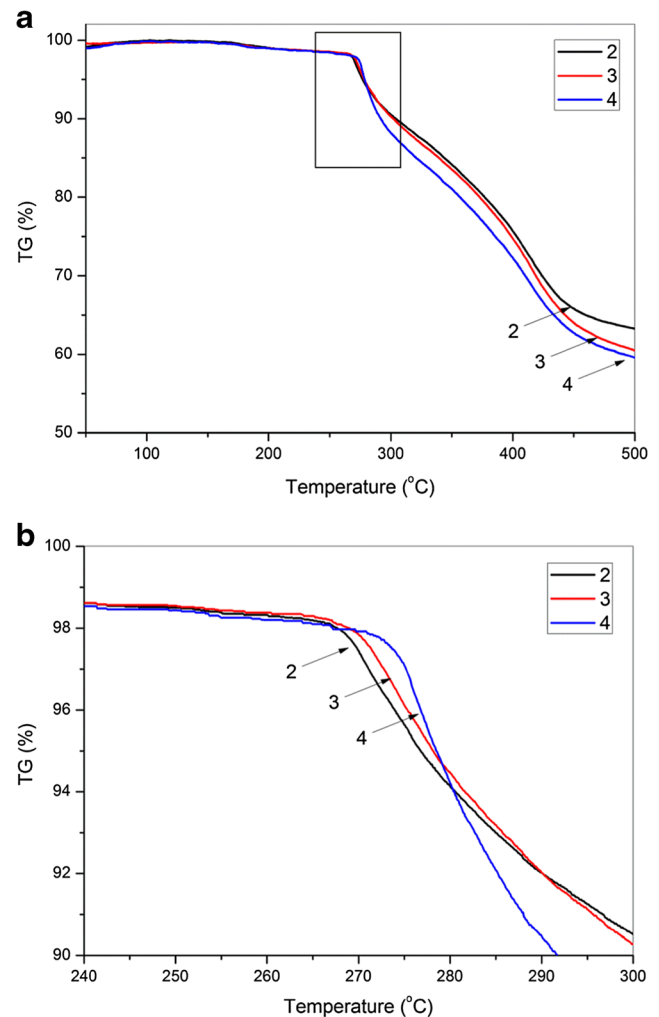
**Fig. 9**  $H$  and  $\pi$  values of the PAN fiber samples

Figure 7 shows the changes in crystallinity  $C$  and crystal size  $L$  of the PAN fibers during the spinning process.  $C$

increases step by step from an initial 51.91 % (sample no. 1) to a final 67.64 % (sample no. 4), whereas  $L$  changes slightly during the first two stages and then increases significantly during the next two stages. After drying,  $L$  increases from 4.2 nm to 6.1 nm. After steam stretching,  $L$  increases further to 7.7 nm. This shows that drying and steam stretching play important roles in the formation and growth of the crystalline structure of PAN fibers. During the drying step, both external and internal water are removed from the PAN fibers by heating. This eliminates the hindrance exerted by water molecules, meaning that the PAN chains can pack more closely together through thermal motion during the drying step, resulting in substantial crystal formation and growth. In other words, a heat-induced crystallization mechanism occurs. During the steam stretching step, a high draw ratio was applied to the PAN fibers. The PAN chains were oriented along the fiber axis by tensile stress, simultaneously inducing further crystallization. As a result,  $C$



**Fig. 10a–b** DSC curves of PAN fibers, obtained under a nitrogen atmosphere. **a** The full curves. **b** Local enlargements of the curves to facilitate comparison



**Fig. 11a–b** TG curves of PAN fibers, as obtained under a nitrogen atmosphere. **a** The full curves. **b** Local enlargements of the curves to facilitate comparison

and  $L$  both increase significantly during this stage, with the PAN fibers mainly undergoing an orientation-induced crystallization mechanism.

### Evolution of the degree of chain orientation in the PAN fibers during the spinning process

Figure 8 shows the azimuthal XRD patterns at  $2\theta=17^\circ$  of the PAN fiber samples obtained at different stages during the spinning process. All of the patterns show a symmetrical peak. The coagulated PAN fibers in sample no. 1 show very little chain orientation, as the azimuthal XRD pattern is a very wide and weak peak. After the spinning process, the peaks become narrower and stronger with each stage. This means that the PAN fibers become increasingly oriented.

The degree of orientation  $\pi$  can be characterized in terms of the  $H$  of the azimuthal XRD pattern (Eq. 4). As shown in Fig. 9,  $\pi$  increases significantly during the two stretching stages (bath stretching, draw ratio=4.5; steam stretching, draw ratio=2.2). After bath stretching,  $\pi$  increases from 61.2 % to 81.6 %. After steam stretching,  $\pi$  increases further to about 90 %, resulting in highly oriented PAN fibers. During the drying step, no stretching is applied to the fiber (draw ratio=1.0). Correspondingly,  $\pi$  barely increases. It can be inferred that  $\pi$  is closely related to stretching. The fibrils and chains in

the PAN fiber can only be oriented under the tension provided by stretching. Thus, stretching is very important for enhancing  $\pi$ , and a large  $\pi$  is necessary to obtain PAN fibers with high tensile strength that can be used in the preparation of high-performance carbon fibers.

### Effect of supramolecular structure on the thermal properties of the PAN fibers

Figure 10 shows DSC curves of three PAN fiber samples (nos. 2, 3, and 4), obtained under a nitrogen atmosphere. All of the PAN fiber samples exhibit a sharp and narrow exothermic peak, which is mainly attributed to cyclization reactions of nitrile groups [25]. These cyclization reactions lead to the formation of a heat-stable ladder structure through the oligomerization of  $-C\equiv N$  groups to  $-C=N$  groups [26]. The differences between these DSC curves are more readily apparent in the local enlargement shown in Fig. 10b. The peak maxima for the three PAN fiber samples are located at about 269.5 °C, 270.8 °C, and 274.8 °C, respectively. As the perfection of the supramolecular structure of the PAN fibers increases, the exothermic peak tends to move to higher temperatures. This indicates that the cyclization reactions are more difficult to carry out when the PAN chains are packed in a more ordered manner. The high order of the supramolecular structure restricts

**Fig. 12** Stress–strain curves of the PAN fiber samples

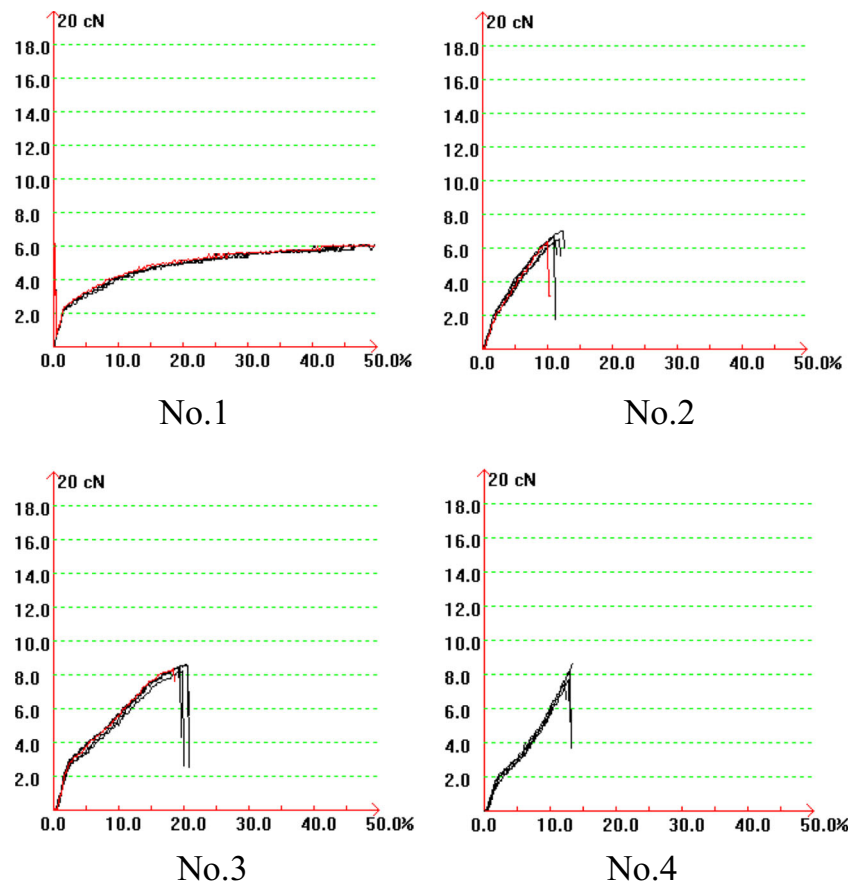




**Table 2** Mechanical properties of the PAN fibers

Sample	Elongation		Tensile strength		Initial modulus	
	ET (%)	CV (%)	TS (cN/dtex)	CV (%)	IM (cN/dtex)	CV (%)
No. 1	>50.0	–	–	–	28.2	9.8
No. 2	11.3	7.4	2.4	10.5	53.0	12.0
No. 3	19.8	4.4	3.2	6.0	73.0	8.9
No. 4	12.9	3.7	6.2	8.6	125.9	7.5

the thermal mobility of the PAN chains, and it is this thermal mobility that permits the cyclization of nitrile groups.

Figure 11 presents TG curves of three PAN fiber samples (nos. 2, 3, and 4), obtained under a nitrogen atmosphere. The weight losses shown in the TG curves are mainly due to the thermal decomposition of PAN chains, which is generally used to evaluate the thermal stability of PAN fibers [26]. Unexpectedly, as the perfection of the supramolecular structure increases, the thermal stability of the PAN fibers tends to decrease at high temperatures. As shown in Figs. 7 and 9, PAN fiber sample no. 4 has the highest degree of crystallinity and orientation. However, it always has the lowest residual weight from about 280 °C to 500 °C. A local enlargement of the TG curves from 240 °C to 300 °C is shown in Fig. 11b. As can be seen in Fig. 11, PAN fiber sample no. 4 exhibits the greatest thermal stability among all the samples below 280 °C. Thermal stabilization of PAN fibers is generally carried out below 280 °C to obtain a homogeneous and controllable stabilized structure. Thus, the perfection of the supramolecular structure seems to help prevent the thermal decomposition of PAN chains during thermal stabilization. This may be attributed to the existence of stronger intermolecular interactions among PAN chains in the highly oriented PAN fibers.

#### Effect of supramolecular structure on the mechanical properties of the PAN fibers

Figure 12 shows the stress–strain curves of the PAN fiber samples, and their mechanical properties are listed in Table 2. As can be seen in Fig. 12, there are striking differences among the four PAN fiber samples. PAN fiber sample no. 1 has a gentle stress–strain curve, while the other PAN fiber samples all have steep stress–strain curves. As the perfection of the supramolecular structure of the PAN fibers increases, the mechanical properties of the fibers tend to improve. As shown in Table 2, PAN fiber sample no. 4 has the highest tensile strength (6.2 cN/dtex) and the highest initial modulus (125.9 cN/dtex), followed by PAN fiber sample no. 3 and then PAN fiber sample no. 2. This demonstrates that supramolecular structure

has a significant effect on the mechanical properties of the PAN fibers.

#### Conclusions

In the present work, highly oriented polyacrylonitrile (PAN) fibers which could be used in the preparation of high-performance carbon fibers were prepared via a wet spinning process. The supramolecular structure—i.e., the degree of crystallinity, crystal size, and crystallite orientation—of the PAN fibers was investigated by XRD, DSC, and TG. Results indicated that the crystalline structure of the PAN fibers is pseudohexagonal, with only two-dimensional order in the transverse direction. In order to obtain a more reproducible value for the relative degree of crystallinity  $C$ , the Gupta–Singhal method was modified by assuming that  $C$  can be obtained by measuring the area under resolved peak 1 ( $2\theta \sim 17^\circ$ ), not the combined area under resolved peaks 1 and 3. The highly oriented PAN fibers were found to have higher values of  $C$  and  $L$  than the unoriented PAN polymer, which was attributed to the higher degree of orientation of the chains. Drying and steam stretching were shown to play important roles in the formation and growth of the crystalline structure of PAN fibers.  $L$  increased significantly during these two stages, which involved a heat-induced crystallization mechanism and an orientation-induced crystallization mechanism, respectively. The degree of orientation ( $\pi$ ) was closely related to the degree of stretching.  $\pi$  increased significantly during the two stretching stages (bath stretching and steam stretching), indicating that the fibrils and chains in PAN fibers can only be oriented under the tension produced by stretching. Increasing the perfection of the supramolecular structure restricted the cyclization of nitrile groups but also helped to prevent the thermal decomposition of PAN chains during thermal stabilization. The mechanical properties of PAN fibers were significantly enhanced by the increased perfection of the supramolecular structure.

**Acknowledgements** The authors would like to thank Prof. Dr. Phillip H. Geil at the University of Illinois for his valuable suggestions, and they acknowledge the financial support provided by the National Natural Science Foundation of China (no. 21404111).

## References

1. Huang X (2009) Fabrication and properties of carbon fibers. *Materials* 2:2369–2403
2. Liu Y, Kumar S (2012) Recent progress in fabrication, structure, and properties of carbon fibers. *Polym Rev* 52:234–258
3. Frank E, Steudle LM, Ingildeev D, Sprl JM, Buchmeiser MR (2014) Carbon fibers: precursor systems, processing, structure, and properties. *Angew Chem Int Ed* 53:5262–5298
4. Quan L, Zhang H, Xu L (2015) Orientation and thermal properties of carbon nanotube/polyacrylonitrile nascent composite fibers. *J Polym Res*. doi:10.1007/s10965-015-0769-4
5. Wang B, Zhao C, Xiao S, Zhang J, Xu L (2012) Effect of the aggregation structure on the thermal shrinkage of polyacrylonitrile fibers during the heat-treatment process. *J Appl Polym Sci* 125: 3545–3551
6. Bohn CR, Schaeffgen JR, Statton WO (1961) Laterally ordered polymers: polyacrylonitrile and poly(vinyl trifluoroacetate). *J Polym Sci* 55:531–549
7. Hinrichsen G (1973) On the origin of order–disorder in drawn polyacrylonitrile. *J Appl Polym Sci* 17:3305–3321
8. Holland VF, Mitchell SB, Hunter WL (1962) Crystal structure and morphology of polyacrylonitrile in dilute solution. *J Polym Sci* 62: 145–151
9. Klement JJ, Geil PH (1968) Growth and drawing of polyacrylonitrile crystals grown from solution. *J Polym Sci Part A-2*(6): 1381–1399
10. Henrici-Olivé G, Olivé S (1979) Molecular interactions and macroscopic properties of polyacrylonitrile and model substance. *Chem Adv Polym Sci* 32:123–152
11. Warner SB, Uhlmann DR (1979) Oxidative stabilization of acrylic fibres. Part 3: Morphology of polyacrylonitrile. *J Mater Sci* 14: 1893–1900
12. Bashir Z, Rastogi S (2005) The explanation of the increase in slope at the  $T_g$  in the plot of  $d$ -spacing versus temperature in polyacrylonitrile. *J Macromol Sci Part B* 44:55–78
13. Bashir Z (2001) The hexagonal mesophase in atactic polyacrylonitrile: a new interpretation of the phase transitions in the polymer. *J Macromol Sci Part B* 40:41–67
14. Bai Y, Wang C, Lun N, Wang Y, Yu M, Zhu B (2006) HRTEM microstructures of PAN precursor fibers. *Carbon* 44:1773–1778
15. Yu M, Wang C, Bai Y, Zhu B, Ji M, Xu Y (2008) Microstructural evolution in polyacrylonitrile fibers during oxidative stabilization. *J Polym Sci Part B Polym Phys* 46:759–765
16. Ouyang Q, Chen Y, Zhang N, Mo G, Li D, Yan Q (2011) Effect of jet swell and jet stretch on the structure of wet-spun polyacrylonitrile fiber. *J Macromol Sci Part B* 50:2417–2427
17. Liu XD, Ruland W (1993) X-ray studies on the structure of polyacrylonitrile fibers. *Macromolecules* 26:3030–3036
18. Chae HG, Minus ML, Kumar S (2006) Oriented and exfoliated single wall carbon nanotubes in polyacrylonitrile. *Polymer* 47: 3494–3504
19. Gupta AK, Singhal RP (1983) Effect of copolymerization and heat treatment on the structure and X-ray diffraction of polyacrylonitrile. *J Polym Sci Part B Polym Phys* 21:2243–2262
20. Hinrichsen G (1972) Structural changes of drawn polyacrylonitrile during annealing. *J Polym Sci Part C* 38:303–314
21. Bell JP, Dumbleton JH (1971) Changes in the structure of wet-spun acrylic fibers during processing. *Text Res J* 41:196–203
22. Murthy NS, Minor H (1990) General procedure for evaluating amorphous scattering and crystallinity from X-ray diffraction scans of semicrystalline polymers. *Polymer* 31:996–1002
23. Mikolajczyk T, Rabiej S, Bogun M (2006) Analysis of the structural parameters of polyacrylonitrile fibers containing nanohydroxyapatite. *J Appl Polym Sci* 101:760–765
24. Matta VK, Mathur RB, Bahl OP, Nagpal KC (1990) Crystallinity of PAN precursors. *Carbon* 28:241–243
25. Ouyang Q, Wang H, Cheng L, Sun Y (2007) Effect of boric acid on the stabilization of poly(acrylonitrile-co-itaconic acid). *J Polym Res* 14:497–503
26. Ju A, Guang S, Xu H (2014) A high performance carbon fiber precursor containing ultra-high molecular weight acrylonitrile copolymer: preparation and properties. *J Polym Res* 21:569. doi:10.1007/s10965-014-0569-2